Characterization of the Growth of 2D Protein Crystals on a Lipid Monolayer by Ellipsometry and Rigidity Measurements Coupled to Electron Microscopy

Catherine Vénien-Bryan,* Pierre-François Lenne,# Cécile Zakri,# Anne Renault,# Alain Brisson,§ Jean-François Legrand,¶ and Bruno Berge#

*Institut de Biologie Structurale Jean-Pierre Ebel (CEA-CNRS), 38027 Grenoble cedex 1, France; #Laboratoire de Spectrométrie Physique, Université J. Fourier Grenoble I, BP 87, 38402 St Martin d'Hères, France; §Department of Chemistry/Biophysical Chemistry, University of Groningen, NL-9747 AG Groningen, The Netherlands; and ¶SI3M (UMR 585 CEA-CNRS-Université J. Fourier), DRFMC, 38054 Grenoble cedex 9, France

ABSTRACT We present here some sensitive optical and mechanical experiments for monitoring the process of formation and growth of two-dimensional (2D) crystals of proteins on a lipid monolayer at an air-water interface. The adsorption of proteins on the lipid monolayer was monitored by ellipsometry measurements. An instrument was developed to measure the shear elastic constant (in plane rigidity) of the monolayer. These experiments have been done using cholera toxin B subunit (CTB) and annexin V as model proteins interacting with a monosialoganglioside (GM1) and dioleoylphosphatidylserine (DOPS), respectively. Electron microscopy observations of the protein-lipid layer transferred to grids were systematically used as a control. We found a good correlation between the measured in-plane rigidity of the monolayer and the presence of large crystalline domains observed by electron microscopy grids. Our interpretation of these data is that the crystallization process of proteins on a lipid monolayer passes through at least three successive stages: 1) molecular recognition between protein and lipid-ligand, i.e., adsorption of the protein on the lipid layer; 2) nucleation and growth of crystalline patches whose percolation is detected by the appearance of a non-zero in-plane rigidity; and 3) annealing of the layer producing a slower increase of the lateral or in-plane rigidity.

INTRODUCTION

Interest in the technique of two-dimensional (2D) crystallization of proteins bound to a lipid monolayer at the air-water interface has increased considerably during the past few years (Uzgiris and Kornberg, 1983; Kornberg and Darst, 1991; Brisson et al., 1994). The domains of applications extend from structural biology to biosensors.

After transfer of 2D crystals to electron microscope grids, structural analysis may be performed by electron crystallography. Some 2D protein crystals are sufficiently well-ordered to give near-atomic resolution (Henderson et al., 1990; Kühlbrandt et al., 1994; Avila-Sakar and Chiu, 1996). Two-dimensional protein crystals have also been used for the seeding and epitaxial growth of 3D protein crystals (Edwards et al., 1994). More recently it has been possible to analyze 2D protein crystals in situ by using grazing incidence x-ray diffraction (Haas et al., 1995; Lenne et al., in preparation).

Up to now, ~30 soluble proteins have been crystallized by using surface-bound affinity ligands (Uzgiris and Kornberg, 1983; Mosser et al., 1992; Célia et al., 1994) or electrostatic interactions (Darst et al., 1989; Schultz et al., 1990; Olofsson et al., 1994). A more recent extension of this technique exploits the interaction between metal coordinated-lipid and polyhistidine tagged protein (Kubalek et al., 1994; Barklis et al., 1997; Vénien-Bryan et al., 1997) or naturally occurring surface histidines (Frey et al., 1996).

The limiting step in structural studies of 2D crystals is the production of large highly ordered crystals. To understand and possibly improve the mechanism of formation and growth of 2D crystals we have developed an approach combining optical, mechanical, and structural techniques. The process of adsorption of the protein on the lipid surface was monitored by ellipsometry. The ellipsometry signal is mainly sensitive to the density and thickness of the layer. As ellipsometry is not sensitive to the lateral crystalline order, we have designed an experiment for measuring the shear elastic constant of the monolayer that allows us to monitor, in real time, the kinetics of shear rigidity. The local structure of the protein-lipid domains was investigated by electron microscopy following standard procedures. This study was performed using as model proteins cholera toxin B subunit (CTB) and annexin V, which have been previously studied extensively (Mosser and Brisson, 1991; Mosser et al., 1992; Olofsson et al., 1994). The CTB interacts with a cell membrane receptor, a monosialoganglioside (GM1), and annexin V interacts with dioleoylphosphatidylserine (DOPS). These ligand lipids are included in the lipid monolayer. In this paper we describe the effect of the lipid composition (ratio ligand lipid/diluting lipid, nature of the diluting lipid) and the protein concentration on the crystallization process.

Received for publication 15 October 1997 and in final form 28 January 1998.

Address reprint requests to Dr. Catherine Vénien-Bryan, Institut de Biologie Structurale Jean-Pierre Ebel (CEA-CNRS), 41 avenue des Martyrs, 38027 Grenoble cedex 1, France. Tel.: 33-4-7688-4568; Fax: 33-4-7688-5494; E-mail: venien@ibs.fr.

© 1998 by the Biophysical Society

0006-3495/98/05/2649/09 $2.00

MATERIALS AND METHODS

Phospholipids and proteins

Stock solutions of dioleoyl phosphatidylcholine (DOPC, Avanti Polar Lipids and Sigma), dilauroyl phosphatidylcholine (DLPC, Sigma), dioleoyl phosphatidylserine (DOPS, Sigma), and monosialoganglioside (GM1, Sigma) were kept in chloroform at −20°C under nitrogen gas. The working solutions were prepared in chloroform/hexane 1:1 (v/v) at a final lipids concentration of 500 μM. Ligand lipids (GM1 or DOPS) were mixed with diluting lipids including DOPC or DLPC at various final ratios of GM1/diluting lipid of 1:3, 1:4, 1:5, 1:20, 1:40, and 1:80 (mol/mol) when used with CTB or DOPS/DOPC of 1:4 (mol/mol) when used with annexin V.

Cholera toxin B subunit (CTB, Sigma) was diluted from 3 to 45 μg/ml in buffer A (170 mM NaCl, 0.75 mM NaN_3, 0.25 mM EDTA, 20 mM Tris-HCl, pH 7.3). Annexin V (a gift from Boehringer Ingelheim) was diluted at 15 μg/ml in buffer B (2mM $CaCl_2$, 100 mM NaCl, 3mM NaN_3, 50 mM Tris-HCl, pH 7.5).

Ellipsometry and surface tension

Ellipsometry has already been used for the study of adsorption of proteins under lipid monolayers (see Andree et al., 1990). In our experiments a laser beam (λ = 670 nm) is used at an incidence angle θ close to the Brewster angle ($\theta_{Brewster} - 1°$). After reflection on the surface of water (Fig. 1) the beam goes through an acoustic birefringence modulator, which adds a small sinusoidal phase difference at 50 kHz, then through a quarter-wave plate and a motorized analyzer whose rotation is precisely measured. The signal of a photodiode can be analyzed with a lock-in detector, whose output serves as a feedback voltage to find the correct position of the analyzer rotation. The analyzer thus automatically rotates toward the extinction position. A computer measures this rotation at regular time intervals. The phase difference δ between the vertical and horizontal polarizations is determined. The analyzer rotation has to be multiplied by two to obtain the ellipsometric angle δ, related to the phase difference between vertical and horizontal beam polarizations. Basically δ, the ellipsometric angle, is proportional to the amount of protein adsorbed at the interface.

The surface tension was measured in the same trough (4×8 cm^2) with the Wilhelmy method using a 1 cm-wide filter paper. For each working lipid solution, the surface pressure of lipids was recorded by successive addition, so that the exact amount of lipid required to obtain a fully dense monolayer and the maximum pressure that lipids can sustain are known. We then systematically worked with a slight excess (15%) compared to this value. The surface pressure of lipids at saturation gives a constant value of typically 48 mN/m, the protein adsorption adding no more lateral pressure.

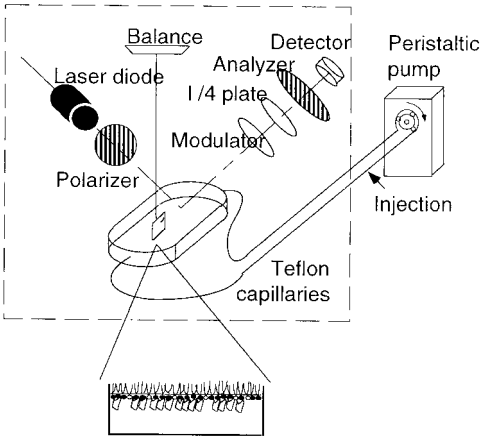

FIGURE 1 Schematic representation of the ellipsometry and surface tension setup. The dotted line represents a polystyrene box enclosing the entire experiment.

The following procedure was used: a lipid monolayer was spread at the air-water interface (typically a few tens of microliters of a working lipid solution at 500 μM in chloroform/hexane 1:1, v/v). Once equilibrium was reached, (~10 min), proteins were injected into the subphase by using small capillaries. A good homogeneity of the protein concentration in the trough was ensured using a peristaltic pump shown in Fig. 1 (switched on for 10 min after injection of the protein). This did not perturb the ellipsometric measurements. A large polystyrene box was used to avoid temperature fluctuations during the measurements.

Measurement of the shear elastic constant

The shear elastic constant μ is defined by the formula

$$\sigma_{xy} = 2\mu\, \mathbf{u}_{xy} \quad (1)$$

where σ is the strain tensor and $\mathbf{u}$ is the deformation tensor (Landau and Lifchitz, 1969). The experiment allowing a direct measurement of the lateral rigidity of the monolayer is described in detail elsewhere (Zakri, 1997). The principles and detailed implementation of our experimental setups are described in the Appendix and Fig. 6. Briefly, a float containing a small magnet is carefully placed in the middle of the trough, in contact with the monolayer. A magnetic field applies a torque on the float, inducing its rotation around the vertical axis. We then directly measured the resistance that the monolayer opposes to the rotation of the float. Unlike other experimental setups (Abraham et al., 1983a,b; Miyano et al., 1983; Krägel et al., 1994a,b), there is no physical link between the outside and the float torsion (no torsion wire). This allows high sensitivities such that the applied deformation is very small, below $\mathbf{u}_{xy} \sim 10^{-7}$. A similar device was used for studying the rheology of soap films (Bouchama and di Meglio, 1996). Our approach is innovative because for the first time we use the device for monitoring 2D crystallization of proteins.

The experimental procedure was usually as follows. We first spread the lipid layer containing the ligand lipids. This layer, a 2D liquid, did not offer any detectable resistance to shear flow and the response was indeed indistinguishable from the pure subphase response. We then recorded the amplitude and phase of the mechanical response at a fixed frequency, usually 5 Hz, as a function of time. After complete stabilization, the protein was injected into the subphase. The homogeneity of the solution was completed using a peristaltic pump as described for ellipsometry experiments. We then followed the kinetics of the rigidification up to stabilization. The amplitude and phase of the float angular motion were then recorded as a function of the frequency. We also varied the strength of the excitation in order to check the linearity of the response (see Appendix).

All the experiments were performed at room temperature. As much as possible ellipsometry and rigidity measurements were carried out in parallel. Systematically, at the end of each experiment we transferred the layer onto electron microscopy grids.

Electron microscopy

Carbon-coated electron microscope grids were placed on top of the monolayer, withdrawn after a few minutes' adsorption, rinsed with distilled water, and negatively stained with 2% (w/v) uranyl acetate for 30 s. Negatively stained specimens were examined in a Zeiss 10C operating at 80 kV. Micrographs were recorded on Kodak SO 163 film under low-dose conditions and at a nominal magnification of 40,000×.

RESULTS

Adsorption and crystallization of CTB on a lipid monolayer: presentation of a standard case

We first present the standard case: the lipid composition was 4 molecules of DOPC for 1 of GM1. The concentration of CTB in the subphase was 5 μg/ml after injection. Fig. 2

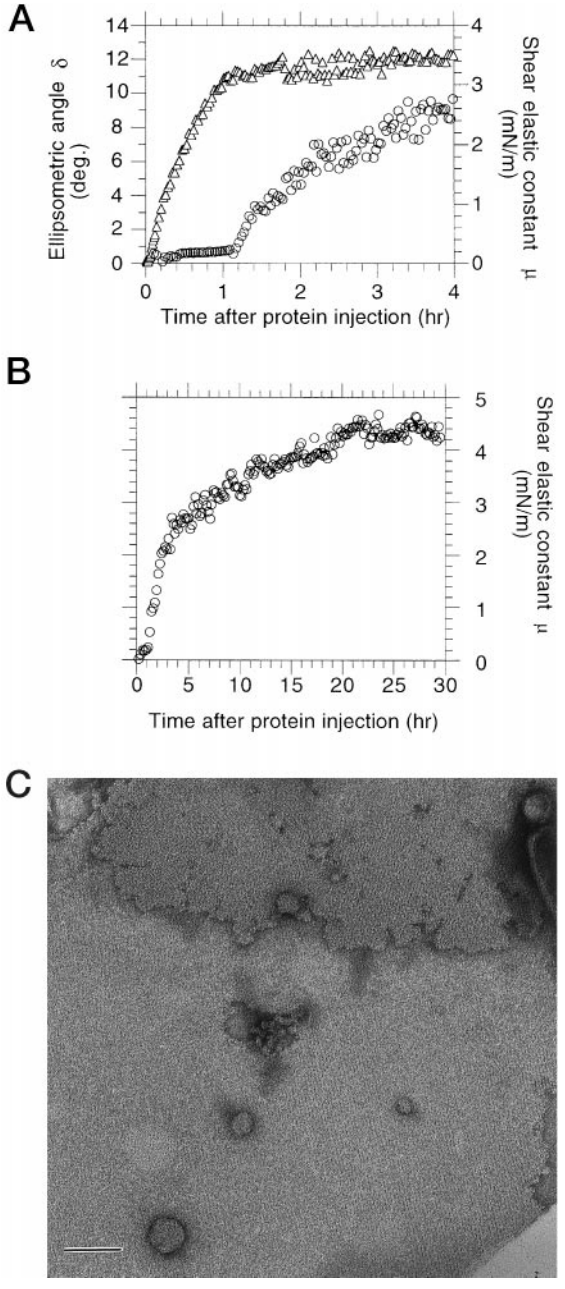

FIGURE 2 A standard case with CTB (5 μg/ml) and GM1/DOPC 1:4. (*A*) Ellipsometric angle δ (*triangle*) and shear elastic constant μ (*circle*) versus time. The measurements are done simultaneously in different troughs; see text for details. (*B*) Elastic constant μ during the whole experiment. The origin of times corresponds to the injection of the protein in the subphase. (*C*) Electron microscopy showing large areas of crystals observed after transfer onto an electron microscope grid at the end of the experiment. The bar represents 100 nm.

A shows the ellipsometric angle and the shear elastic constant as a function of time. The ellipsometric angle δ is proportional to the quantity of protein adsorbed to the lipid monolayer. The lipid layer contribution to δ was $\sim 8°$ and has been subtracted in Fig. 2 *A*. This measurement shows that adsorption started immediately after injection. Half-maximal adsorption was reached after $\sim$25 min. Adsorption appears to be completed after 1 h and the ellipsometric angle reached $\delta = 12 \pm 0.5°$. The evolution of the shear elastic constant as a function of time is shown on the same figure. The shear rigidity was estimated at a fixed frequency of 5 Hz. The appearance of a rigidity is only observed after a delay of $\sim$1 h. The rigidity is expected to appear after crystallites have grown sufficiently to touch each other. A non-zero shear rigidity corresponds, then, to the percolation of 2D crystals over the whole area between the float and the edge of the trough. After 3 h the shear elastic constant reached $\sim$2 mN/m. Fig. 2 *B* shows the same experiment on longer time scales. It is clear that after 3 h the elastic constant still increased, but at a slower rate, and continues to increase for $>$10 h. This corresponds to another regime, where annealing of some defects occurs. This could be coalescence of neighboring crystallites or thinning of the grain boundary zone between individual crystals.

After transfer onto electron microscope grids, at the end of the experiments numerous 2D crystal domains were visible. The size of the domains was $\sim$0.5 to 1 μm, as seen Fig. 2 *C*.

These physical techniques, ellipsometry and shear elastic measurements, require a larger trough, typically 4×8 cm^2 and 4.8 cm diameter, respectively; that is much larger than the small 3-mm wells used for preparing specimens for electron microscopy. To economize on material, low protein concentrations were routinely used (from 3 to 15 μg/ml). Under these conditions all the kinetics measured were slower than in previous work.

Influence of the lipid composition on the adsorption and crystallization of cholera toxin B

Ratio of GM1/DOPC

The ligand lipid GM1 was mixed with DOPC in chloroform/hexane 1:1. The working solution (500 μM) was prepared at various final ratios of GM1/DOPC 1:3 and 1:5 (mol/mol) for the higher GM1 ratios and 1:20, 1:40, and 1:80 (mol/mol) for the lower GM1 ratios. The protein concentration was kept constant at 15 μg/ml during all these experiments.

For the higher GM1 ratios (GM1/DOPC 1:3 and 1:5), the ellipsometry angle at saturation was almost constant ($11.6 \pm 0.5°$). At ratio 1:5 (as shown in Fig. 3 *A*), the protein layer exhibits a maximum compacity. The observed time at which half the maximum ellipsometric angle (maximum absorption) occurred was $t_{1/2} = 200$ s. The measured shear elastic constant for these higher GM1 ratios is 5 ± 0.5 mN/m (data not shown but similar to Fig. 2 *B*). As in the standard case, numerous 2D crystal domains were visible with a size of 0.5–1 μm.

For the lower ratios of dilution (GM1/DOPC: 1:20, 1:40, and 1:80), the ellipsometric angle varied according to these ratios (Fig. 3 *A*). GM1/DOPC (1:20) gave a saturation value of $8 \pm 0.5°$. The adsorbed surface density of the protein was

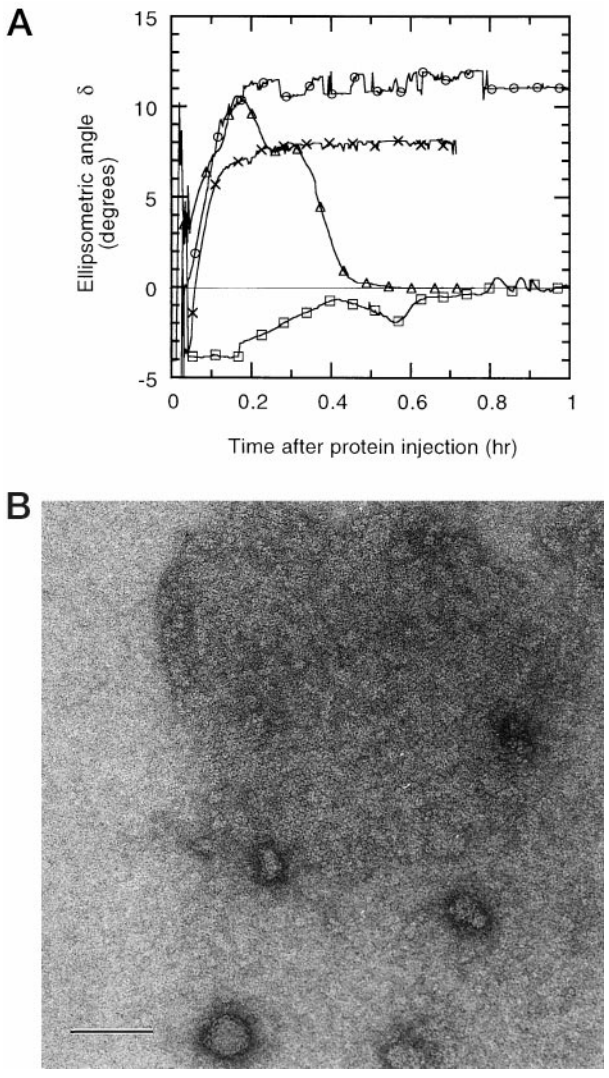

FIGURE 3 Influence of lipid composition using CTB at 15 μg/ml. (*A*) Ellipsometric angle versus time. Lipid contribution has been subtracted. The ratios GM1/DOPC are circle, 1:5; cross, 1:20; triangle, 1:40; square, 1:80. (*B*) Electron microscopy of hexagonal patch after only few hours incubation with GM1/DOPC 1:20. The bar represents 100 nm.

lower than what was obtained with the higher GM1 ratio. The GM1/DOPC ratio 1:40 gave large fluctuations of the ellipsometric angle interpreted as the presence of moving patches of protein at the air-water surface with various degrees of compaction. At GM1/DOPC 1:80 the adsorption was very low. For all experiments using the lower GM1 ratios (1:20, 1:40, and 1:80), the protein adsorbed did not oppose any resistance to lateral flow. The value of the rigidity was null during the whole experiment (not shown). This is correlated with the observation of electron microscopy grids: the large crystalline domains were no longer present for these ratios. Only with the ratio 1:20 could one observe 2D microcrystals of 0.1–0.3 μm (Fig. 3 *B*). These microcrystals mainly gave a diffraction pattern of a hexagonal close-packed assembly.

DLPC instead of DOPC

The influence of DLPC as a diluting lipid was tested. Experiments of adsorption and crystallization of CTB using DLPC instead of DOPC as the diluting lipid were carried out. DLPC contains saturated lauroyl tails (C12). The GM1/DLPC ratio was 1:4. The ellipsometric angle value obtained after saturation with a CTB concentration of 15 μg/ml was comparable to the value found with GM1/DOPC (data not shown), but the shear elastic response (2.5 $\pm$ 0.5 mN/m), was low compared with 5.5 $\pm$ 1 mN/m with GM1/DOPC. Nevertheless, increasing the concentration of CTB to 45 μg/ml gives a value of ~6 mN/m.

The observation of the electron microscope grids after transfer at the end of the experiments revealed a few crystalline domains, but they were not as numerous as when the DOPC was used.

Influence of the protein concentration on the adsorption and crystallization of cholera toxin B

Fig. 4 *A* shows the effect of protein concentration (3, 5, and 10 μg/ml) on the adsorption on a GM1/DOPC 1:4 monolayer. The ellipsometric angle at saturation was $\delta = 11.6 \pm 0.5°$; this value was independent of the protein concentration. The kinetics varied with concentration. The $t_{1/2}$ at which half the maximum ellipsometric angle occurred was

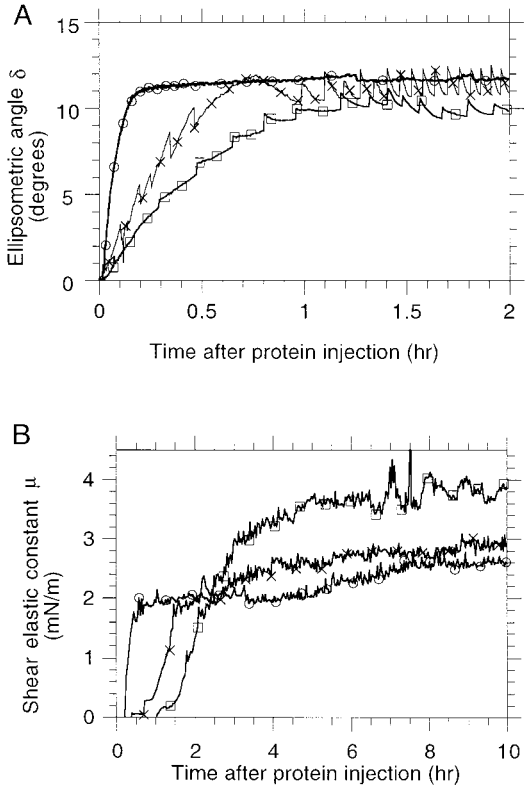

FIGURE 4 Influence of the concentration of proteins. Three different concentrations of CTB were used: square, 3 μg/ml; cross, 5 μg/ml; circle, 10 μg/ml. The lipid ratio is GM1/DOPC 1:4. (*A*) Ellipsometry; (*B*) rigidity.

200, 1000, and 2000 s for 10 μg/ml, 5 μg/ml, and 3 μg/ml, respectively. It is notable that even at a concentration of 3 μg/ml the quantity of protein was estimated to be largely sufficient to cover the surface of the trough.

The kinetics of appearance of lateral crystalline order varied also with the protein concentration, as shown in Fig. 4 *B*. After a delay of a few minutes to one hour, depending on the protein concentration, the shear elastic constant increased and the $t_{1/2}$ at which the maximum values were found was 1800, 4000, and 5000 s for 10 μg/ml, 5 μg/ml, and 3 μg/ml, respectively. In this set of experiments another protein batch was used. It might explain the reason why we get lower values of the shear rigidity at saturation.

For these three CTB concentrations the observation of the electron microscopy grids showed large crystalline domains similar to those presented in Fig. 2 *C*.

Annexin V

Similar experiments were performed with annexin V, an anticoagulant protein that binds to DOPS in the presence of calcium.

The protein concentration was kept at 15 μg/ml and the DOPS/DOPC ratio at 1:4. Fig. 5 *A* presents the time-dependent evolution of the ellipsometric angle and the shear elastic constant. At equilibrium the ellipsometric angle stays constant at the value $\delta = 10.4 \pm 0.5°$. As for the CTB, the process of adsorption appeared first, in ~2–3 min, then the crystallization process was much slower (Fig. 5 *B*); the shear elastic constant was 2.8 ±1 mN/m after 30 h. The very long time scales observed in this case are explained by the low protein concentration. Electron microscopy observations show large crystalline domains, as one can see in Fig. 5 *C*.

DISCUSSION

The experiments presented here show that the formation of crystals takes place in three successive stages: 1) molecular recognition between protein and lipid-ligand, i.e., adsorption of the protein on the lipid layer as monitored by ellipsometric measurements. 2) Nucleation and growth of crystalline patches. At some point the patches touch their neighbors such that a non-zero lateral rigidity appears on macroscopic shear modulus. Crystals are also observed on electron microscope grids. 3) A slow annealing, revealed by a slight increase of the shear elastic constant over time constants from 10 to 40 h. Each point is discussed below.

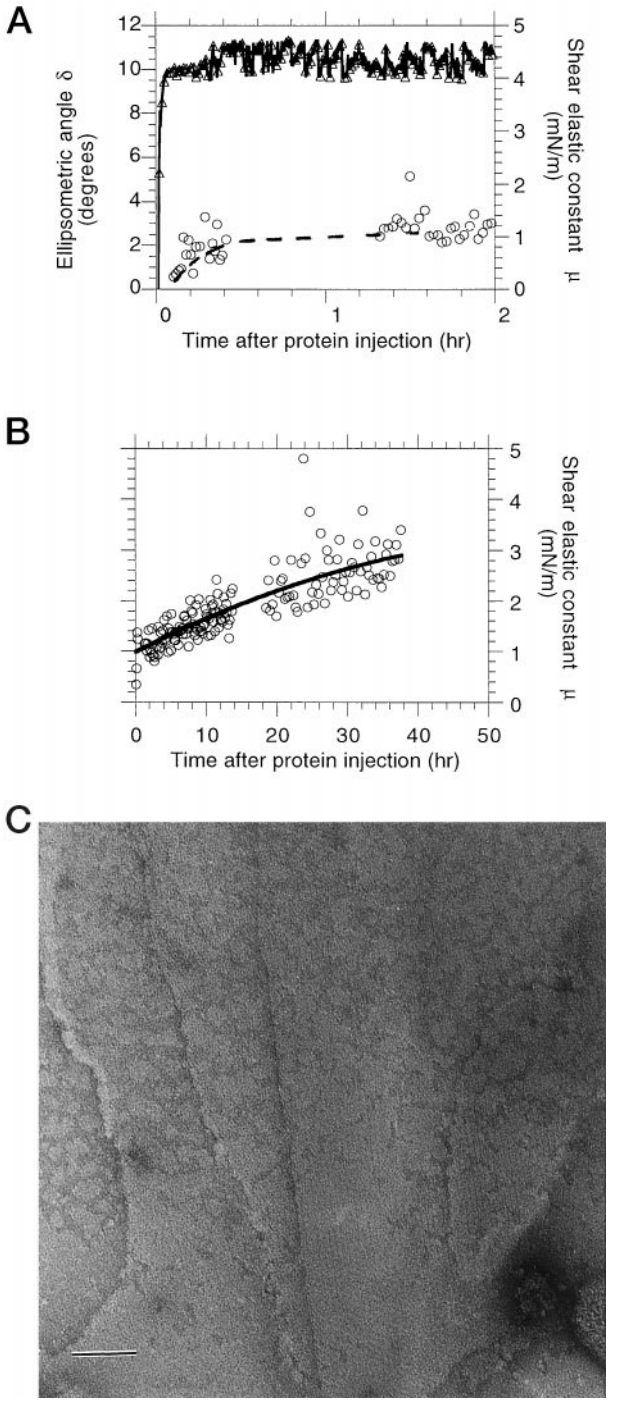

FIGURE 5 Similar experiments with annexin V at 15 μg/ml using a mixture of DOPC/DOPS 4:1. (*A*) Ellipsometry (*triangle*) and shear elastic constant (*circle*) versus time. (*B*) Shear elastic constant versus time showing the long-term evolution. (*C*) Electron microscopy observations of the monolayer transferred on electron microscope grids. The bar represents 100 nm.

Measurements of the lateral rigidity (appearance of crystals)

Although ellipsometry is an accurate technique that allows access to the kinetics of adsorption of the protein on the lipid monolayer, it gives no indication on the crystalline order of the protein adsorbed. That is the reason why we decided to perform mechanical measurements. This gives access to the kinetics of rigidification of the monolayer. There is clearly a delay before the onset of rigidification (1 h, Fig. 2). We interpret a non-zero value of the shear rigidity as reflecting the percolation of 2D crystals over the area

between the float and the edge of the trough. Then another slower process appears; this long-term evolution with slower kinetics is due to a phenomenon of annealing of the 2D crystals. This might involve thinning of the grain boundaries and/or coalescence.

One can address another issue concerning the mechanical experiment: does the shear elastic constant measurement bring any information about the protein-protein lateral interactions? In other words, is the value obtained by a macroscopic measurement also valid at a microscopic scale? When working with fatty alcohol monolayers we have clearly shown a dramatic difference between the macroscopic shear elastic constant measured with the same apparatus as presented here (a few mN/m), and the microscopic constant (300 mN/m), deduced from the line shape of the Bragg peak of the 2D crystals (Zakri et al., 1997). Although solid, the alcohol monolayers underwent plastic deformation to such an extent that the mechanical rigidity was so small that we could not attribute the values to a pure solid. The results obtained with protein 2D crystals seem much clearer. We did not see any evidence for plastic deformations as demonstrated by the good linearity between stress and strain (Fig. 8) and the curves of Figs. 7 and 8 show that the response is equivalent to a perfect elastic solid. Also, there is an excellent agreement between the non-zero values of the shear elastic constant and presence, quality, and size of the crystalline patches on the electron microscopy grids. Nevertheless, the values measured ($\mu \sim 6$ mN/m) are still small and suggest that the elasticity of the polycrystalline layers is dominated by soft grain boundaries between the crystalline patches. Another explanation of this low value could be an effect of buckling in the third dimension. This out-of-plane deformation could then produce an apparent shear modulus much smaller than the real one. This point of discussion should make us cautious in interpreting the absolute values of rigidities.

Ellipsometric measurements

The binding of the CTB is stimulated by GM1. The CTB is composed of 5 B-subunits of each 11,600 MW. The total weight is 58,000. Fig. 3 shows that the maximum compaction of the protein on the lipid monolayer was found with a ratio of GM1/DOPC from 1:3 to 1:5 and was inductive to crystallization. A ratio of 1:20 and lower did not induce the compaction necessary for obtaining large crystalline domains. The ratio giving an optimal adsorption lies between 1:20 and 1:5. This value is in agreement with an estimate one can make taking into account 1) the area occupied by the absorbed molecule of CTB (28 nm^2), which corresponds to ~40 molecules of lipids; and 2) the 5 GM1 binding site of CTB (Merritt et al., 1994). Therefore, the minimum estimated ratio (GM1/diluting lipid) needed for the complete adsorption of the CTB is 1:8, which is in agreement with the experimental value found between 1:20 and 1:5 (see also Mosser and Brisson, 1991).

Superimposition of several crystalline layers on the electron microscope grids is a striking feature. Are they already present in situ or are they the result of the transfer to electron microscopy grids? We addressed these questions by measuring the ellipsometric angle while increasing the concentration of lipids and then proteins. With lipids alone, when the saturation value (corresponding to the saturation of the interface by lipids measured by surface tension) was reached, this value stayed constant even if an excess of lipids was added. The lipids at this stage did not spread spontaneously, but stayed in some undissolved lenses that eventually formed "reservoirs" on the Teflon trough edges. When proteins were added, the ellipsometric angle increased until a saturation value, which was constant even if the protein was largely in excess in the solution (see Fig. 4). These measurements show clearly that at the interface there is only one layer of lipids and most probably one layer of proteins. The laser beam is a few millimeters in diameter, giving a macroscopic value of the ellipsometric angle. On a macroscopic scale there is probably one layer of protein, but we cannot rule out the possibility of the presence of 2–3 microscopic superimposed layers of crystalline protein in some zones. In that case these superimposed areas should be quite rare and limited in size, because they were not detected by ellipsometry. Therefore, the transfer onto electron microscope grids is probably at the origin of the superimposition of several layers (up to seven in some cases). It is worth noting that the transfer may also induce deformation of the crystals.

Nature of the diluting lipid

Other conditions are necessary for the crystallization process to take place. Among them the nature of the diluting lipid is important. It is known that the crystallization of CTB does not appear when the lipid layer is made of pure GM1 (Ribi et al., 1988; Mosser and Brisson, 1991). GM1 is a saturated lipid with a large hydrophilic headgroup and at room temperature does not form stable and fluid monolayers leading to crystallization. CTB-GM1 2D crystals are observed only when unsaturated diluting lipids are mixed with GM1. DOPC is made of unsaturated oleoyl fatty acyl chains (C_{18}) which provide the monolayer fluidity allowing the lateral and rotational mobility of the bound protein necessary for its self-organization and formation of optimal intermolecular contacts and efficient packing within the crystal. Unsaturated chains are subjected to degradation. This chemical reaction often leads to polymerization between tails of lipids and reduces the fluidity and formation of crystals. We did not observe this kind of denaturation in the particular experiments presented in this paper. However, because we plan to study the 2D crystals at the air-water interface with an x-ray beam, we were concerned by this problem of degradation of lipids, which leads to a lack of fluidity. We decided to test DLPC as diluting lipids. Although DLPC is saturated, the shortness of the saturated

lauroyl chain (C_{12}) makes it fluid at room temperature. We experimentally checked that the mixture of DLPC/GM1 is perfectly fluid, using the mechanical experiment. Obviously this lipid does not easily induce crystallization. A possible explanation for the difficulty for obtaining crystals is the differences of the chain lengths between GM1 (C_{18}) and DLPC (C_{12}), which could introduce a spontaneous curvature of the film that reduces the mobility of GM1. Another explanation is that compared to DOPC, DLPC may phase-separate more readily in mixtures with the receptor lipid GM1.

CONCLUSION

In conclusion, we raise a few points. We measured a non-zero in-plane shear rigidity (resistance to flow) at the end of experiments performed with CTB and annexin V layers. This is strong evidence that the crystals exist at the water surface, before transfer onto electron microscope grids (but not a proof, a solid can be disordered!). Ellipsometry and surface tension ensured that the lipid and probably the protein form a single layer at the interface. We have shown that the formation of these crystals occurs in the three successive stages described above.

These results validate the technique of ellipsometry and shear rigidity measurements for studying crystallization in two dimensions. These techniques are now available for testing on other systems, for instance His-tag protein binding to metal chelating lipids.

APPENDIX: LATERAL RIGIDITY MEASUREMENT

A schematic view of the setup is shown Fig. 6. A small circular Teflon trough (48 mm diameter) containing 8 ml of the subphase covered by the monolayer under study is used (in gray on the figure). At the center of the trough, a small piece of paraffin-coated aluminum disk (~10 mm diameter) is floating at the water surface and is surrounded by the monolayer whose rigidity is measured. The float contains a small magnet (black rectangle on the figure), and a small vertical mirror; the total weight is ~32 mg. In order to avoid the drift of the float away from the trough center, we apply an inhomogeneous d.c. magnetic field parallel to the horizontal component of the earth magnetic field, using a small solenoid just above the center of the trough. The contribution of the solenoid and the earth magnetic fields are $B_0 = 6.4 \pm 0.5 \cdot 10^{-5}$ T at the level of the float. B_0 is equivalent to a torsion wire by giving an equilibrium position and orientation to the float. This device has the advantage of avoiding any physical link with the float. Measurements are straightforward; a current in the large peripheral Helmholtz coils applies a torque to the small magnet in the float, which tends to force it to rotate around the vertical axis. This adds a small alternating magnetic field $B_\perp$, which is horizontal but perpendicular to the direction of the continuous magnetic field, B_0. The absolute value of $B_\perp$ is typically $10^{-4} \cdot B_0$, the frequency ranging from 0.01 Hz to 100 Hz. The value of the magnetic moment of the magnet in the float is $m = 8 \pm 1.5 \cdot 10^{-4}$ A · m^2. The amplitude of rotation of the float, measured with a laser beam reflected on the small mirror, is directly related to the rigidity of the monolayer: the motion of the float is restricted by a monolayer behaving like a solid.

The very special feature of this setup is the high angular sensitivity that allows the measurements using very small deformations of the solid superficial layer, down to shear deformations as small as $\mathbf{u}_{xy} \sim 10^{-7}$. The stiffness of the restoring torque due to B_0 is equivalent to a monolayer having a shear rigidity of ~0.16 mN/m. We then are able to detect a shear elastic response of real monolayers with a value as small as this order of magnitude, 0.1 mN/m. The whole setup is protected from drafts and attached to the main wall of our building, ensuring excellent antivibration properties. Injection of the protein using capillaries does not perturb the shear elastic measurements. Note that when a torque is applied to the float the deformation of the monolayer is inhomogeneous, i.e., this deformation is larger close to the float, where the strain is applied, than far from it. In this paper we consider the deformation $\mathbf{u}_{xy}$ close to the float, given by:

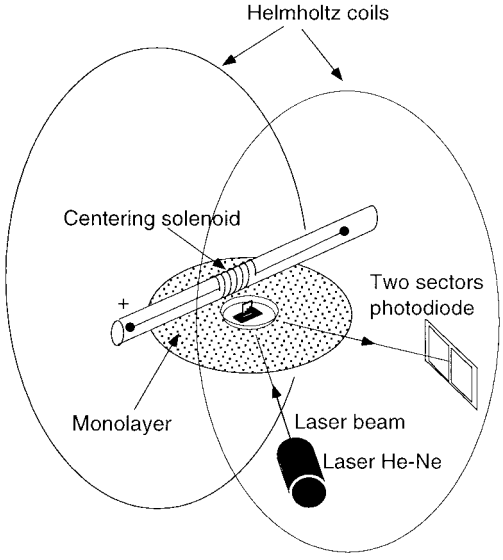

FIGURE 6 Schematic representation of the setup built for the measurement of the lateral rigidity of the monolayers under study. The large coils at the exterior of the experiment serve to apply a torque to the float. In response to this torque, the float rotates around the vertical axis. The amplitude of rotation is dependent on the restoring forces applied by the monolayer under shear deformation.

$$u_{xy} = 2\theta \frac{b^2}{b^2 - a^2} \tag{2}$$

where θ is the float rotation angle in radians and a and b are the float and trough radii, respectively. The stress σ_{xy} is directly related to the magnetic field applied by the Helmholtz coil:

$$\sigma_{xy} = \frac{mB_\perp}{2\pi a^2} \tag{3}$$

The amplitude of rotation (Fig. 7 *A, circles*) and the phase difference with the excitation (Fig. 7 *B, circles*) of the float without monolayer is first measured as a function of frequency of excitation. The system behaves like a simple harmonic oscillator with a resonance frequency

$$\omega_0^2 = \frac{B_0 m}{J} \tag{4}$$

where J is the inertia momentum of the float. A fit of the data (Fig. 7, *solid line*) allows us to determine ω_0 and J, which is then inserted in the equation of motion. Lipids alone at the surface give a mechanical response identical to a pure water subphase; the lipid layer is indeed in a liquid state, offering no detectable resistance to shear. After injection of the CTB the response values exhibit a time evolution. Upon full equilibration, i.e., 25 h incubation, the mechanical response measurements—amplitude of rotation and phase difference with the excitation—are recorded as a function of the frequency (Fig. 7 *A* and *B, squares*). We observe that the float rotation amplitude is ~50× smaller compared with the value without monolayer.

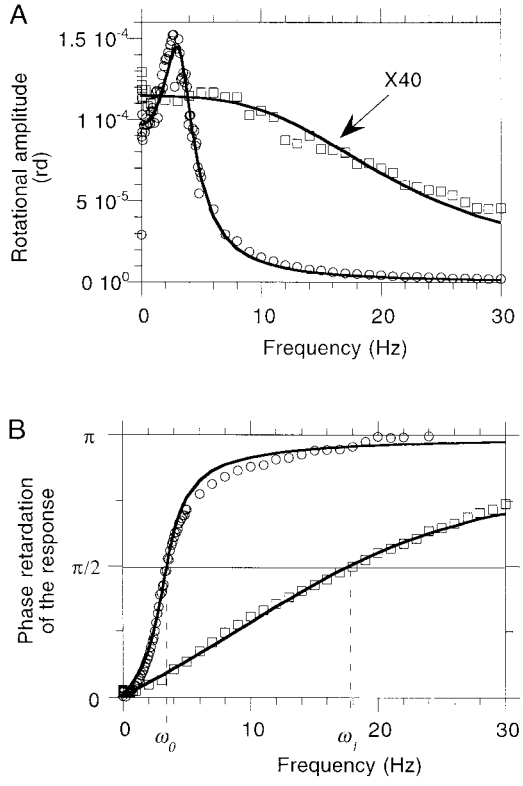

FIGURE 7 Amplitude (*A*) and phase (*B*) of angular motion of the float, measured as a function of the frequency of the excitation in the absence of monolayer (*circle*) and in the presence of a rigid layer of proteins CTB after 25 h incubation (*square*). Both are for the same excitation. Note that in the presence of the rigid layer, the rotation of the float is strongly restricted in such way that the amplitude of rotation has been multiplied by ~40 in order to appear on the same scale as the control in the absence of the monolayer. On the phase plot (*B*) the position of the resonance frequencies ω_0 and ω_1 are shown. The ratio of lipid is GM1/DOPC 1:4. The concentration of CTB is 10 μg/ml.

The system behaves like a damped harmonic oscillator and the fit shows a shift of the resonance frequency. This is what we expect for a monolayer behaving mechanically like a pure solid. Indeed, a simple derivation gives the expected value of the resonance frequency ω_1 (Zakri, 1997):

$$\omega_1^2 = \omega_0^2 + \frac{4\pi a^2 b^2}{(b^2 - a^2)J}\,\mu \qquad (5)$$

where a is the float radius, b is the trough radius, and μ is the shear elastic constant of the monolayer. Fig. 8 shows the linearity of the deformation $\mathbf{u}_{xy}$ as a function of the stress σ_{xy}, which confirms that the protein monolayers are in the linear elastic regime, as postulated by Eq. 1. The curve shows no evidence for nonlinearity or plastic deformations, which means that the monolayers are not broken (only deformed), even under the maximum stress used here.

In conclusion, the mechanical properties of the crystallized protein monolayers correspond perfectly and unambiguously to an elastic solid, down to very low frequencies (below 0.1 Hz). To our knowledge, this case is much less ambiguous than comparable measurements performed on usual Langmuir monolayers, where it is often necessary to introduce a characteristic time at which the mechanical response changes from liquid-like to solidlike. The cleanliness of the experimental results we present here and the simplicity of the data analysis give us confidence in the measured shear elastic constant μ.

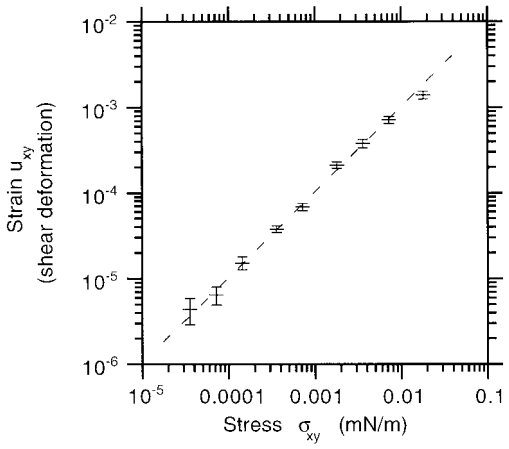

FIGURE 8 Log-log plot of the shear deformation of a rigid monolayer of CTB, estimated directly from the rotation of the float, as a function of the applied shear stress. This experiment is performed at a fixed frequency of 5 Hz. The ratio of lipids is GM1/DOPC 1:4. The concentration of CTB is 10 μg/ml.

We thank Dr. R. Wade for valuable discussions and support all along the project, and Hélène Bussidan for her help with some ellipsometric measurements. This is publication number 531 of the Institut de Biologie Structurale, Jean-Pierre Ebel (CEA-CNRS).

REFERENCES

Abraham, B. M., K. Miyano, S. Q. Xu, and J. B. Ketterson. 1983a. Centro-symmetric technique for measuring shear modulus, viscosity and surface tension of spread monolayers. *Rev. Sci. Instrum.* 51:213–219.

Abraham, B. M., K. Miyano, J. B. Ketterson, and S. Q. Xu. 1983b. Anomalous melting properties of some classical monolayers systems. *Phys. Rev. Lett.* 51:1975–1978.

Andree, H. A. M., C. P. Reutelingsperger, R. Hauptmann, H. C. Hemker, W. T. Hermens, and G. M. Willems. 1990. Binding of vascular anticoagulant α (VACα) to planar phospholipid bilayers. *J. Biol. Chem.* 265:4923–4928.

Avila-Sakar, A. J., and W. Chiu. 1996. Visualization of β-sheets and side-chain clusters in two-dimensional periodic arrays of streptavidin on phospholipid monolayers by electron crystallography. *Biophys. J.* 70: 57–68.

Barklis, E., J. McDermott, S. Wilkens, E. Schabtach, M. F. Schmid, S. Fuller, S. Karanjia, Z. Love, R. Jones, Y. Rui, X. Zhao, and D. Thompson. 1997. Structural analysis of membrane-bound retrovirus capsid proteins. *EMBO J.* 16:1199–1213.

Bouchama, F., and J. M. di Meglio. 1996. Two-dimensional rheology of soap films. *J. Phys. Condens. Matter*. 8:9525–9529.

Brisson, A., A. Olofsson, P. Ringler, M. Schmutz, and S. Stoylova. 1994. Two dimensional crystallization of protein on planar lipid films and structure determination by electron crystallography. *Biol. Cell*. 80: 221–228.

Célia, H., L. Hoermann, P. Schultz, L. Lebeau, V. Mallouh, D. Wigley, J. Wang, C. Mioskowski, and P. Oudet. 1994. Three-dimensional model of *Escherichia coli* gyrase B subunit crystallized in two dimensions on novobiocin-linked phospholipid films. *J. Mol. Biol.* 236:618–628.

Darst, S. T., E. W. Kubalek, and R. D. Kornberg. 1989. Three-dimensional structure of *Escherichia coli* RNA polymerase determined by electron crystallography. *Nature*. 340:730–732.

Edwards, A. L., S. A. Darst, S. A. Hemming, Y. Li, and R. D. Kornberg. 1994. Epitaxial growth of protein crystals on lipid layers. *Nat. Struct. Biol.* 1:195–197.

Frey, W., W. Schief, D. Pack, C. Chen, A. Chilkot, P. Staylon, V. Vogel, and F. Arnold. 1996. Two-dimensional protein crystallization via metal-ion coordination by naturally occurring surface histidines. *Proc. Natl Acad. Sci. USA* 93:4937–4941.

Haas, H., G. Brezesinski, and H. Mohwald. 1995. X-ray diffraction of a protein crystal anchored at the air-water interface. *Biophys. J.* 68: 312–314.

Henderson, R., J. Baldwin, T. Ceska, F. Zemlin, E. Beckmann, and K. Downing. 1990. Model for the structure of bacteriorhodopsin based on high-resolution electron cryo-microscopy. *J. Mol. Biol.* 213:899–929.

Kornberg, R. D., and S. Darst. 1991. Two-dimensional crystals of proteins on lipid layers. *Curr. Opin. Struct. Biol.* 1:642–646.

Krägel, J., S. Siegel, and R. Miller. 1994a. Surface shear rheological studies of protein adsorption layers. *Prog. Colloid. Polym. Sci.* 87: 183–187.

Krägel, J., S. Siegel, R. Miller, M. Born, and K.-H. Schano. 1994b. Measurement of interfacial shear rheological properties: an automated apparatus. *Colloids and Surfaces*. 91:169–180.

Kubalek, E., S. Le Grice, and P. Brown. 1994. Two-dimensional crystallization of histidine-tagged HIV-1 reverse transcriptase promoted by a novel nickel-chelating lipid. *J. Struct. Biol*. 113:117–123.

Kühlbrandt, W., D. N. Wang, and Y. Fujiyhoshi. 1994. Atomic model of plant-harvesting complex by electron crystallography. *Nature*. 367: 614–621.

Landau L. D., and E. M. Lifchitz. 1969. Elasticité. Ed Mir, Moscow.

Merritt, E. A., S. Safarty, F. van den Akker, C. L'hoir, J. A. Martial, and W. G. J. Hol. 1994. Crystal structure of cholera toxin B-pentamer bound to receptor GM1 pentasaccharide. *Protein Sci.* 3:166–175.

Miyano, K., B. M. Abraham, J. B. Ketterson, and S. Q. Xu. 1983. The phases of insoluble monolayers: comparison between the surface pressure-molecular area (P-A) diagram and shear modulus measurements. *J. Chem. Phys.* 78:4776–4777.

Mosser, G., and A. Brisson. 1991. Conditions of two-dimensional crystallization of cholera toxin B-subunit on lipid films containing ganglioside GM1. *J. Struct. Biol.* 106:191–198.

Mosser, G., V. Mallouh, and A. Brisson. 1992. A 9 Å two-dimensional projected structure of cholera toxin B-subunit-GM1 complexes determined by electron crystallography. *J. Mol. Biol.* 226:23–28.

Olofsson, A., V. Mallouh, and A. Brisson. 1994. Two-dimensional structure of membrane-bound annexin V at 8 Å resolution. *J. Struct. Biol.* 113:199–205.

Ribi, H. O., S. D. Ludwig, K. L. Mercier, G. K. Schoolnik, and R. D. Kornberg. 1988. Three dimensional structure of cholera toxin penetrating a lipid membrane. *Science*. 239:1272–1276.

Schultz, P., H. Célia, M. Riva, S. A. Riva, P. Colin, R. D. Kornberg, A. Sentenac, and P. Oudet. 1990. Structural study of the yeast RNA polymerase A: electron microscopy of lipid-bound molecules and two-dimensional crystals. *J. Mol. Biol.* 216:353–362.

Uzgiris, E., and R. Kornberg. 1983. Two-dimensional crystallization technique for imaging macromolecules with application to antigen-antibody-complement complexes. *Nature*. 301:125–129.

Vénien-Bryan, C., F. Balavoine, B. Toussaint, C. Mioskowski, E. Hewat, B. Helme, and P. Vignais. 1997. Structural study of the response regulator HupR from *Rhodobacter capsulatus*. Electron microscopy of 2D crystals on a nickel-chelating lipid. *J. Mol. Biol*. 247:687–692.

Zakri, C. 1997. Etude de la fusion-cristallisation de monocouches de l-alcools a la surface de l'eau: mesures d'élasticité latérale par diffraction de rayons X et par une méthode mécanique. Ph.D. Thesis. University of Grenoble I, France.

Zakri, C., A. Renault, J. P. Rieu, M. Vallade, B. Berge, J. F. Legrand, G. Vignault, and G. Grübel. 1997. Determination of the in-plane elastic tensor of crystalline decanol monolayers on water by x-ray diffraction. *Phys. Rev. B.* 55:14163–14172.